



Intranasal delivery of lipid-based nanosystems as a promising approach for brain targeting of the new-generation antiepileptic drug perampanel

Sara Meirinho^{a,b}, Márcio Rodrigues^{a,b,c}, Catarina L. Ferreira^{a,b}, Rui Caetano Oliveira^{d,e,f}, Ana Fortuna^{g,h}, Adriana O. Santos^{a,b}, Amílcar Falcão^{g,h}, Gilberto Alves^{a,b,*}

^a CICS-UBI – Health Sciences Research Center, University of Beira Interior, Av. Infante D. Henrique, 6200-506 Covilhã, Portugal

^b Faculty of Health Sciences, University of Beira Interior, Av. Infante D. Henrique, 6200-506 Covilhã, Portugal

^c CPIRN-UDI-IPG-Center for Potential and Innovation of Natural Resources, Research Unit for Inland Development, Polytechnic of Guarda, 6300-559 Guarda, Portugal

^d Pathology Department, Centro Hospitalar e Universitário de Coimbra, Coimbra, Portugal

^e Biophysics Institute, Faculty of Medicine, University of Coimbra, 3000-548 Coimbra, Portugal

^f Coimbra Institute for Clinical and Biomedical Research (iCBR) Area of Environment Genetics and Oncobiology (CIMAGO), Faculty of Medicine, University of Coimbra, 3000-548 Coimbra, Portugal

^g Laboratory of Pharmacology, Faculty of Pharmacy, University of Coimbra, Pólo das Ciências da Saúde, Azinhaga de Santa Comba, 3000-548 Coimbra, Portugal

^h CIBIT/ICNAS – Coimbra Institute for Biomedical Imaging and Translational Research, University of Coimbra, Pólo das Ciências da Saúde, Azinhaga de Santa Comba, 3000-548 Coimbra, Portugal

ARTICLE INFO

Keywords:

Brain delivery
Lipid-based nanosystems
Intranasal administration
Perampanel
Pharmacokinetics
Epilepsy

ABSTRACT

Perampanel (PER), a new-generation antiepileptic drug effective against different types of seizures, has already demonstrated a potential in *status epilepticus* therapy. Considering the growing interest of intranasal (IN) administration for nose-to-brain delivery, PER could be envisioned as a good candidate for this route, especially if formulated in a lipid-based nanosystem. With that purpose, a hydrophobic formulation (FO1.2) and a self-microemulsifying drug delivery system (SMEDDS) (FH5) loaded with PER were developed and characterized. Following PER IN administration (1 mg/kg) to mice, its pharmacokinetics was characterized and compared with intravenous and oral routes. Histopathological toxicity was also examined after a 7-day repeated dose study. FH5 homogeneously formed nanodroplets upon dispersion (20.07 ± 0.03 nm), showing a sustained *in vitro* PER release profile up to 4 h. By IN route, PER brain delivery was more extensive with FH5 (C_{max} and AUC of 52.32 ng/g and 190.35 ng.h/g for FO1.2; 93.87 ng/g and 257.75 ng.h/g for FH5). Maximum brain concentration and total brain exposure were higher than those obtained after oral dosage, with maximum PER concentrations reached significantly faster than post-oral administration (15 min vs 2 h). An improvement in PER plasmatic concentration was also obtained, demonstrated by high relative bioavailability values (134.1% for FH5 and 107.8% for FO1.2). PER absolute plasma bioavailability after IN delivery was 55.5% for FH5 and 44.6% for FO1.2, ensuring a somewhat improved targeting of PER to the brain by the IN route compared to the IV route. No signs of toxicity were found by histopathologic evaluation. Results suggest that IN administration of PER might be a feasible and safe approach for acute and chronic epilepsy management, especially using delivery systems as SMEDDS.

Abbreviations: AEDs, antiepileptic drugs; AMPA, α -Amino-3-hydroxy-5-methyl-4-isoxazolepropionic acid; AUC, area under the drug concentration-time curve; BBB, blood-brain barrier; C_{last} , last quantifiable drug concentration; C_{max} , maximum (or peak) drug concentration; CNS, central nervous system; CYP, cytochrome P450; DTE (%), drug targeting efficiency percentage; DTP (%), direct transport percentage; F, absolute bioavailability; FH, hydrophilic formulation; FO, oily formulation; F_{rel} , relative bioavailability; H&E, hematoxylin and eosin; HPLC, high-performance liquid chromatography; IN, intranasal; IV, intravenous; k_{el} , terminal elimination rate constant; log P, octanol-water partition coefficient; MRT, mean residence time; PAS, periodic acid-Schiff; PDI, polydispersity index; PER, perampanel; O/W, oil-in-water; SMEDDS, self-microemulsifying drug delivery system; SEM, standard error of the mean; $t_{1/2el}$, elimination half-life; t_{max} , time to reach maximum (or peak) drug concentration; W/O, water-in-oil.

* Corresponding author at: Faculty of Health Sciences, CICS-UBI – Health Sciences Research Center, University of Beira Interior, Av. Infante D. Henrique, 6200-506 Covilhã, Portugal.

E-mail address: gilberto@fcsaude.ubi.pt (G. Alves).

<https://doi.org/10.1016/j.ijpharm.2022.121853>

Received 12 February 2022; Accepted 19 May 2022

Available online 25 May 2022

0378-5173/© 2022 Elsevier B.V. All rights reserved.

1. Introduction

Epilepsy is a chronic neurological condition that affects nearly 50 million people worldwide (World Health Organization, 2019). However, one-third of patients fail to respond to the available antiepileptic drugs (AEDs), developing refractory epilepsy (Biase et al., 2018; Li et al., 2021; Patsalos, 2015). This is one of the main reasons for continuing to develop new generation AEDs with better efficacy and safety, as it is perampanel (PER), a highly potent third generation AED (LaPenna and Tormoehlen, 2017; Patsalos, 2015). There are also some serious medical convulsive conditions characterized by long persisting seizures, namely refractory *status epilepticus*, which are associated with brain injury and high mortality rates. In these clinical states, there is an urgent need to stop seizures, being required emergency drug therapy as early as possible, especially if the seizure lasts longer than 5 min (American Epilepsy Society, 2016; Marawar et al., 2018). In these circumstances, intravenous (IV) benzodiazepines (midazolam, lorazepam or diazepam) followed by IV AEDs (phenobarbital, phenytoin/fosphenytoin, valproic acid or levetiracetam) are still the standard therapeutic approaches (American Epilepsy Society, 2016; Der-Nigoghossian et al., 2019). However, there is an inherent need of specialized assistance for IV administrations. So, a possible alternative that can overcome the drawbacks of AEDs parenteral administration is the intranasal (IN) route, as it allows the self-administration of AEDs in cluster seizures.

In fact, over the recent years, the IN route has proved to be a safe and non-invasive alternative to directly deliver drugs through olfactory and/or trigeminal nerves to cerebrospinal fluid and brain tissues, bypassing the blood–brain barrier (BBB) (Costa et al., 2021; Crowe et al., 2018; Kapoor et al., 2016; Oliveira et al., 2016). This will enable a decrease in drugs systemic distribution along with an avoidance of hepatic first-pass effect, potentially increasing drugs targeting and safety (Kapoor et al., 2016; Oliveira et al., 2016). However, IN route requires either highly potent drugs as benzodiazepines, or high strength formulations that allow the administration of low volumes compatible with the capacity of nasal cavity (Crowe et al., 2018; Kapoor et al., 2016). There are currently some developed IN formulations, as the nasal spray preparations of midazolam (Nayzilam®) and diazepam (Valtoco®) (U.S. Food and Drug Administration, 2020; U.S. Food and Drug Administration, 2019). Both have recently received marketing approval from the Food and Drug Administration as alternatives to standard IV therapies in pre-hospital setting (American Epilepsy Society, 2016). Nevertheless, the two formulations have considerable amounts of organic solvents in their composition, which can lead to local and systemic side effects. Additionally, the risks of respiratory depression and hypotension associated with benzodiazepines' administration, and the decreased efficacy of benzodiazepines in later stages must also be considered (American Epilepsy Society, 2016; Der-Nigoghossian et al., 2019; Strzelczyk et al., 2019).

Thus, alternative AEDs, with unique mechanisms of action, high potency and showing good therapeutic efficacy using lower doses and frequency of administration, can be a reliable option for IN administration (Biase et al., 2018; Patsalos, 2015). Since PER presents all those features, it may be an attractive alternative to be formulated as an IN preparation. Until now, this new generation AED is only available in the form of oral tablets and suspension, being used in a once-daily administration regimen (Chang et al., 2020; European Medicines Agency, 2017; Patsalos, 2015). Due to its high potency, PER shows clinical efficacy with low doses (2–12 mg/day), presenting a plasma therapeutic range in humans of 0.1–1 mg/L (European Medicines Agency, 2017; Food and Drug Administration, 2012; Patsalos, 2015; Reimers and Berg, 2018). Since its approval, PER is indicated as monotherapy or adjunctive therapy in partial-onset seizures, with or without secondary generalization, and as add-on therapy in primary generalized tonic-clonic seizures (Chang et al., 2020; Fogarasi et al., 2020). Evidence also shows that the compliance to PER treatment is associated with a high rate of seizures control and low seizure recurrence, reducing hospitalizations

and emergency visits (Li et al., 2021; Toledano Delgado et al., 2020). Besides, there are clinical reports that suggest PER use in pediatric patients with drug-resistant epilepsy and with tuberous sclerosis or Dravet syndrome, even without being approved for it (Chang et al., 2020; Ikemoto et al., 2019). Another valuable application already subject to research is the use of PER in *status epilepticus*, particularly when used in high doses by nasogastric delivery (Newey et al., 2019; Rahbani et al., 2019; Strzelczyk et al., 2019). However, similarly to IV route, nasogastric administration is also a difficult and invasive approach, which can be also overcome with a possible IN formulation of PER. This is not only more patient-friendly in the treatment of *status epilepticus*, but also enables a decrease in PER administered dose and its associated peripheral side effects, maintaining its efficacy in both chronic and acute therapies.

Bearing in mind the hypothesis of formulating PER as an IN preparation, the use of lipid-based nanosystems can be a feasible alternative to consider. In fact, these systems have been extensively studied as alternative dosage forms for nose-to-brain drug delivery, especially for poor aqueous soluble drugs such as PER. Besides the improvement of drugs bioavailability, lipid-based nanosystems present high biocompatibility and potential for direct drug targeting at therapeutic concentrations, which has turned these systems highly attractive (Costa et al., 2019; Feng et al., 2018). The lipid-based nanosystems have also proved to protect drugs from enzymatic degradation as well as to increase drugs stability in the formulation by maintenance of the lipophilic molecules in a solubilized state (Costa et al., 2019; Feng et al., 2018). Especially considering microemulsions, they can either be oil-in-water (O/W) or water-in-oil (W/O) thermodynamically stable formulations (Costa et al., 2019; Kapoor et al., 2016). Therefore, for lipophilic molecules as PER, it can be assumed that higher oil percentages might increase drug solubility and, consequently, the formulation dosage. The O/W microemulsions have shown to be effective vehicles for lipophilic molecules, being even more common than W/O emulsions. Therefore, the use of self-microemulsifying drug delivery systems (SMEDDS) can be a promising strategy to enhance the delivery of poor aqueous soluble drugs (Yan et al., 2020). SMEDDS are transparent isotropic mixtures of oil, surfactant and co-surfactant (or co-solvent) that spontaneously form fine and homogeneous microemulsions when in contact with aqueous fluids as the nasal mucous (Gupta et al., 2013; Nagaraja et al., 2021). The small droplets lead to an improvement of lipophilic drugs stability, solubility, and absorption, which is translated into an increase in brain bioavailability. Hence, the IN administration of high doses is possible even with the instillation of small volumes compatible with nasal capacity (Nagaraja et al., 2021). Moreover, it is important to consider that, for nose-to-brain delivery, small particle size (≤ 200 nm) and formulation lipophilicity are essential characteristics, which can be easily attained with SMEDDS rather than with pre-formulated microemulsion (Gupta et al., 2013; Yan et al., 2020).

Therefore, given the size (349.4 Da), hydrophobicity (log P 3.7) and water insoluble character (5.6 mg/L) of PER (Law et al., 2018; Meirinho et al., 2021), as well as its pharmacological potency, the present study aimed to properly formulate PER in lipid-based liquid nanosystems to be administered through IN route, possibly directing PER into the brain, bypassing the BBB. To corroborate the potential of this route, single-dose pharmacokinetic characterization of PER after its IN administration to mice, and the comparison with oral and IV administration was herein performed. A 7-day repeated IN dose study was also performed to infer about the safety and effects of PER lipid-based formulations in histopathological characteristics of several tissues (brain, liver, kidneys, lungs and heart).

2. Materials and methods

2.1. Materials

PER (99.9% purity) was received as a gift sample from MSN

Laboratories Ltd. (Hyderabad, India), Fycompa® 0.5 mg/mL oral suspension (Eisai GmbH, Germany) was purchased from a local pharmacy (Covilhã, Portugal) and terbinafine hydrochloride (99.5% purity) was gently provided by Bluepharma (Coimbra, Portugal). Pentobarbital sodium injection solution (Eutasil®) was purchased from Ceva (Libourne, France). Glycerol Monocaprylate, type I (Imwitor® 988) was donated by IOI Oleochemical (Hamburg, Germany). Caprylocaproyl macrogol-8-glycerides (Labrasol® ALF), propylene glycol dicaprylocaprate (Labrafac® PG), propylene glycol caprylate (Capryol® 90), glycerol mono-oleate (Maisine® CC), glycerol mono-oleate type 40 (Pecol™), triglycerides medium-chain (Labrafac™ Lipophile WL 1349) and diethylene glycol monoethyl ether (Transcutol® HP) samples were kindly supplied by Gattefossé (Saint-Piest, France). Castor oil, triglycerides medium-chain (Miglyol® 812), propylene glycol, polyethylene glycol 400 (PEG 400), polysorbate 20 (Tween 20) and polysorbate 80 (Tween 80) were obtained from Acofarma (Barcelona, Spain). Isopropyl myristate (Kollicream® IPM), triacetin (Kollisolv® GTA), macrogolglycerol hydroxystearate (Kolliphor® RH 40), macrogolglycerol ricinoleate (Kolliphor® EL) and macrogol 15 hydroxystearate (Kolliphor® HS 15) were donated by BASF Europe, and glycerol monocaprylocaprate type I (Capmul® MCM) and caprylocaproyl macrogolglycerides (Acconon CC-6) samples were obtained from ABITEC (Columbus, USA). Acetonitrile (HPLC grade), analytical grade triethylamine, 85% *ortho*-phosphoric acid, sodium chloride and sodium hydrogen carbonate, were all acquired from Fisher Scientific (Leicestershire, United Kingdom). Isopropanol (98% purity) and absolute ethanol (99.8% purity) were purchased from Honeywell Riedel-de Haën™ (Seelze, Germany); potassium chloride was purchased from Chem-Lab (Zedelgem, Belgium); monobasic and dibasic sodium phosphate from Acros Organics (Geel, Belgium); magnesium chloride from Labkem (Barcelona, Spain); calcium chloride and magnesium sulphate (MgSO₄) were acquired from Panreac (Barcelona, Spain); hydrochloric acid fuming 37% was bought from Fluka (Seelze, Germany) and sodium chloride solution (NaCl) 0.9% obtained from B. Braun Medical (Queluz de Baixo, Portugal). Ultra-pure water was obtained from a Milli-Q water apparatus, 0.22 µm filter, of Merck (Darmstadt, Germany).

2.2. Solubility assays

The first steps for development of PER IN formulations were taken by combining several oils, surfactants and co-surfactants to prepare either hydrophilic formulations (FH) or oily formulations (FO). That was accomplished considering the qualitative and quantitative composition of micro and nanoemulsions already published for the IN administration of hydrophobic drugs (Abd-Elrasheed et al., 2018; Bahadur and Pathak, 2012; Boche and Pokharkar, 2017; Bshara et al., 2014; Florence et al., 2011; Gupta et al., 2013; Iqbal et al., 2019; Kumar et al., 2008a; Meirinho et al., 2021; Mustafa et al., 2015; Nagaraja et al., 2021; Pires et al., 2020; Ramreddy and Janapareddi, 2019; Rashed et al., 2018; Shah et al., 2018; Law et al., 2018). In some cases, excipients were replaced by others available in our lab and, if justifiable, proportions were also adjusted (Supplementary Tables S1 and S2). The formulations were prepared by weighting together the ingredients of the anhydrous pre-concentrate (oil, surfactant and co-surfactant), followed by addition of the pre-determined aqueous phase percentage. To determine PER solubility in each formula, an excess amount of drug was added to 1 mL of each mixture, vortex-mixing it for 1 min. Then, eppendorfs were shaken for 48 h at 300 rpm in an orbital shaker incubator thermostated at 25 ± 1 °C. Later, the mixtures were centrifuged at 12,300g for 20 min and supernatants were recovered. Finally, before high-performance liquid chromatography (HPLC) analysis (Meirinho et al., 2020), samples ($n = 3$) were submitted to a first 100-fold dilution with methanol followed by a second 100-fold dilution with water/acetonitrile (53:47, v/v).

2.3. Pharmaceutical characterization of intranasal formulations

2.3.1. Viscosity

Viscosity measurements were completed using a Brookfield DV3T cone-plate rheometer and a CP40Z cone spindle (Brookfield Ametek, Massachusetts, USA). The temperature was regulated and kept constant at 20 °C using a thermostated water bath (MultiTemp III Thermostatic Circulator, Thermo Fisher Scientific, New Hampshire, USA). The sample volume of each formulation, loaded or not with PER, was 0.5 mL. Shear rates were gradually increased from the minimum to the maximum torque values and, to minimize viscosity measurement errors, the viscosity considered for each fluid was the plateau value correspondent to the shear rate that reached the maximum torque value (<100%).

2.3.2. pH measurement

The pH of the formulations, with or without PER, was estimated at room temperature ($n = 4$). The pH of 2-fold diluted samples was measured using a calibrated pH meter (Orion Star A211 pH meter, Thermo Fisher Scientific, Indonesia) and compared with the pH of the water used in the sample dilution step.

2.3.3. Particle size and polydispersity index

For each sample, mean particle size and polydispersity index (PDI) were automatically measured in triplicate using a Zetasizer Nano ZS apparatus (Malvern, United Kingdom). Samples were diluted 25- and 100-fold in water and the measurements were made in disposable ultraviolet/visible polymethyl methacrylate cuvettes (Kartell, Noviglio, Italy), at 25 °C. Both parameters were obtained by cumulants' analysis of dynamic light scattering data.

2.3.4. In vitro drug release study

The *in vitro* drug release protocol was adapted from a previously developed method (Pires et al., 2020), performing several preliminary tests to ensure the achievement of experimental sink conditions. These studies were accomplished using horizontal Ussing Chambers (Harvard Apparatus, NaviCyte, Hugstetten, Germany), maintained at 32 °C by a heating bath (Grant Instruments, Cambridge, England). To create the air/liquid interface, membranes composed of hydrophilic polyether sulfone, 0.2 µm pore size (Supor® membrane disc filters, Pall Life Sciences, Michigan, USA) were used.

Each bottom chamber (receptor compartment) was filled with 1.9 mL of a nasal fluid simulant buffer pH 6.5 (nasal pH) composed of monobasic sodium phosphate 7 mM, dibasic sodium phosphate 3 mM, potassium chloride 30 mM, sodium chloride 107 mM, calcium chloride 1.5 mM, magnesium chloride 0.75 mM, and sodium hydrogen carbonate 5 mM (Pires et al., 2020). When chambers were fully assembled ($n = 4$), 100 µL of the buffer was added to the upper side of the membrane and let to stabilize until reaching 32 °C. Then, the nasal fluid simulant buffer in the upper chamber (donor compartment) was replaced by 100 µL of each formulation under study (PER at 1 mg/mL). After 10, 30, 60, 90, 120, 150, 180 and 240 min, samples of 200 µL were taken from each receptor compartment and replaced by the same volume of blank nasal fluid simulant buffer. During the assay, homogenization of the receptor compartment fluid was accomplished with magnetic stirring at 200 rpm.

The positive control of drug release was a 1 mg/mL PER solution in Transcutol and the negative control was an oily solution of PER (1 mg/mL) prepared in Capryol® 90. For HPLC quantification of the PER concentration in each formulation under study (i.e., added to donor compartment), a first 30-fold dilution with Transcutol, followed by a second 30-fold dilution with water/acetonitrile (53:47, v/v) were performed. For PER quantification in each collected sample at receptor compartment, only a 30-fold dilution with water/acetonitrile (53:47, v/v) was performed before injection into the HPLC apparatus.

Drug release parameters were determined considering the PER initial concentration in each assayed formulation. Drug release rates were calculated considering a zero-order kinetic model, represented in its

simplistic form as $Y = kX + b$ (Bruschi, 2015; Singhvi and Singh, 2011), with X representing time in hours, Y the drug release percentage, b the drug release percentage when time is zero, and k the zero-order release constant or, in this case, the release rate of PER from each formulation. For a better uniformization of the obtained results, Y values were normalized by the area of the membrane (0.64 cm^2) used in the assay ($Y = Y/0.64$). A linear regression was then applied using mean normalized Y values for each time point. For the obtained positive control values, late time points that fell out the linear zone were excluded to ensure a fitting into the zero-order model and a further better comparison with the remaining results. To assess if the calculated rates were significantly different between formulations (FH5 vs FO1.2) and between formulations and control solutions (FH5 vs C+ and FO1.2 vs C-), the drug release rates were compared two-by-two using an F-test.

2.4. In vivo studies

2.4.1. Animals

Healthy adult male CD-1 mice, aged between 8 and 10 weeks and weights ranging from 30 to 45 g, were obtained from local certified facilities (Faculty of Health Sciences of University of Beira Interior, Covilhã, Portugal). All animals were housed under controlled environmental conditions (12/12 h light–dark cycles, temperature at $20 \pm 2^\circ \text{C}$ and relative humidity of $50 \pm 5\%$), receiving sterile tap water and standard rodent diet *ad libitum* (4RF21, Mucedola, Italy). The animal experimental protocols were reviewed and approved by the Portuguese National Authority for Animal Health, Phytosanitation and Food Safety (DGAV - Direção Geral de Alimentação e Veterinária), in agreement with the regulations of the European Directive 2010/63/EU.

2.4.2. Preliminary in vivo studies

Hydrophilic formulations (FH) that enabled a higher PER solubility (i.e., FH4, FH5, FH5.4, FH6 and FH29; Supplementary Table S1) were tested in preliminary *in vivo* studies; all these five formulations only contained between 5% and 10% of aqueous phase. In addition, to understand the influence of a higher aqueous percentage (30%), FH28.3 was also preliminary tested, as it achieved higher PER solubility ($6.64 \pm 0.88 \text{ mg/mL}$) comparatively to the PER solubility in other formulations with equivalent or higher aqueous percentages (Supplementary Table S1). Selected FOs that allowed a good PER solubility (i.e., FO1.2, FO2 and FO3) were also assayed in *in vivo* preliminary studies (Supplementary Table S2). All tested formulations allowed an IN administration of 1 mg/kg of PER, using an administration volume of only 5 μL per 30 g of animal weight (Supplementary Tables S1 and S2). For each of the aforementioned formulations, two mice were used per time-point, being anesthetized before the IN administration (see Section 2.4.4). At the predetermined post-dosing times (15 and 60 min), animals were sacrificed, matrices were harvested and, after preparation, subjected to HPLC analysis (see Sections 2.4.4 and 2.4.5). The two formulations that achieved higher brain concentrations and brain/plasma ratios in these preliminary studies were further investigated in single dose complete pharmacokinetic studies in mice (see Section 2.4.4).

2.4.3. Preparation of selected formulations

Based on the solubility assays (Section 2.2) and preliminary *in vivo* studies results (Section 2.4.2), two final IN formulations, one of hydrophobic nature and the other characterized as being a SMEDDS (from now designated as FO1.2 and FH5, respectively), were prepared for administration to mice in single dose pharmacokinetic studies (Section 2.4.4). FH5 pre-concentrate was prepared by combining Miglyol® 812 (10%), Kolliphor® RH40 (40%) and Transcutol HP (40%). FO1.2 was prepared by mixing Capmul MCM (40%), Capryol 90 (27.5%) and Transcutol HP (27.5%). An appropriate amount of PER was then dissolved in the anhydrous pre-concentrates by vortex-mixing and ultrasonic dissolution to achieve a final concentration of 6 mg/mL. Water (10% and 5%, to FH5 and FO1.2, respectively) was finally added

dropwise. Formulations were homogenized by gentle inversion, inspected for particulate matter, and stored at room temperature protected from light until used.

For oral administration, Fycompa® 0.5 mg/mL oral suspension was 5-fold diluted with ultra-pure water to reach a suspension with a final concentration of 0.1 mg/mL, allowing an administration of the 1 mg/kg.

For IV administration, a PER solution was prepared by diluting PER in a mixture of propyleneglycol/NaCl 0.9% solution/ethanol (50:30:20, v/v/v), ensuring fluidity and absence of suspended particles in the final formulation. The final PER concentration was of 0.25 mg/mL and the respective administration dose of 0.5 mg/kg.

2.4.4. In vivo single dose pharmacokinetic studies

The comparative pharmacokinetic studies were carried in 4 groups of male CD-1 mice: the first and second ones received either FH5 or FO1.2 by IN route (5 $\mu\text{L}/30 \text{ g}$ body weight), the third received a slow IV tail vein injection (60 $\mu\text{L}/30 \text{ g}$ of body weight injected over approximately 1 min), while the fourth group was administered by oral route (300 $\mu\text{L}/30 \text{ g}$ using an adequate gavage feeding tube coupled to a syringe). The dose of PER administered by IN and oral routes was 1 mg/kg, while the IV dose was 0.5 mg/kg. With the exception of the mice group receiving oral dosing, all animals were pre-anesthetized with pentobarbital (60 mg/kg) through intraperitoneal injection and kept in a warm environment to avoid hypothermia. After totally anesthetized, for the IN administrations, mice were laid in a supine head-back positioning under a rolled pillow placed in a heating pad coupled with a DC Temperature Controller 40–90-8D (FHC, Maine, USA) (Erdő et al., 2018; Yu et al., 2017). A flexible catheter attached to a 50 μL syringe (Hamilton, Nevada, USA) was inserted 3 to 4 mm into the right nostril. After drug administration, mice were left to recover from anesthesia in a supine position, in a temperature-controlled environment to avoid hypothermia.

At the predetermined time-points after PER administrations (5, 10, 15, 30, 45, 60, 90, 120, 180, 240, 480 and 720 min; $n = 4$ per time-point), if responsive, mice were again subjected to anesthesia, and cardiac puncture was used to collect blood into 1 mL tubes containing K₂-EDTA (BD Vacutainer®). Immediately after the blood collection, brain, liver and kidneys were harvested and gently washed using a 0.9% NaCl solution in order to remove the remaining blood. Blood samples were centrifuged at 3351g for 10 min at 4 °C to obtain plasma samples. Plasma and organs were stored at -20°C protected from light until analysis.

2.4.5. Processing of biological samples and HPLC analysis

Before analysis, plasma samples, brain, liver and kidneys were thawed. The organs were weighed and homogenized in a 1 M sodium phosphate buffer pH 5 (4 mL/g tissue) using an Ultra-turrax® tissue homogenizer (Ika Ultra-Turrax® T25 Basic, Staufen, Germany) and the tissue homogenates were centrifuged at 17,350g for 15 min at 4 °C (Alves et al., 2007).

All quantitative determinations of PER in plasma and tissues homogenate supernatants obtained from the *in vivo* pharmacokinetic studies were performed using a HPLC method fully validated by our research group (Meirinho et al., 2020). Briefly, 100 μL of plasma or tissues homogenate supernatants were spiked with 20 μL of terbinafine (internal standard, 100 $\mu\text{g/mL}$) followed by the addition of 200 μL isopropanol and 100 μL 1 M MgSO₄ in order to induce a salting-out effect. Mixture was vortex-mixed for 1 min and centrifuged at 12,300g for 3 min at room temperature, and the upper organic layer was transferred to a glass tube to be evaporated under gentle nitrogen stream (45 °C). Finally, the dried sample was reconstituted using 200 μL of mobile phase, centrifuged at 12,300g for another 3 min and 20 μL of the remaining supernatant injected in the chromatographic system for PER analysis.

The analysis was carried out using a HPLC system (Shimadzu Corporation, Japan) equipped with a DGU-20A5R automatic degasser, a LC-20AD quaternary solvent pump, a CTO-10AS VP columns oven, an SIL-

20AIGHT refrigerated automatic injector and an RF-20AXS fluorescence detector. Data acquisition and instrumentation were controlled using LabSolutions software (Shimadzu Corporation, Japan). PER and terbinafine were separated using a reverse-phase LiChroCART® Purospher Star column (C₁₈, 55 mm × 4 mm; 3 μm), protected by a LiChroCART® Purospher Star precolumn (C₁₈, 4 mm × 4 mm; 5 μm), both purchased from Merck (Darmstadt, Germany), maintained at 35 °C and flushed at 1 mL/min with a mobile phase composed of ultra-pure water containing 1% (v/v) triethylamine (pH 2.5, adjusted with 85% *ortho*-phosphoric acid)/acetonitrile (53:47, v/v). Detection of PER and internal standard was conducted using two excitation and emission wavelength pairs: 275/430 nm and 254/372 nm, respectively.

2.4.6. Pharmacokinetic and statistical analysis

PER maximum (peak) concentration (C_{max}) in plasma and tissues, and the respective time to reach it (t_{max}) were directly estimated from the experimental data. The remaining pharmacokinetic parameters were calculated from the mean concentration–time profiles (n = 4 per time-point) using WinNonlin v5.2. (Pharsight Co, Mountain View, CA, USA) and non-compartmental analysis. Plasma and tissues concentrations below the lower limit of quantification of the analytical method (1 ng/mL for plasma, brain and kidneys; 2 ng/mL for liver) were considered as zero for the pharmacokinetic analysis. The area under the drug concentration–time curve (AUC) from time zero to the time of the last quantifiable drug concentration (AUC_{0-t}) was calculated based on the linear trapezoidal rule. The AUC from time zero to infinity (AUC_{inf}) was calculated using the formula AUC_{0-t} + (C_{last}/k_{el}), where C_{last} is the last quantifiable drug concentration and k_{el} is the terminal elimination rate constant estimated by a log-linear regression of the terminal segment of each concentration–time profile. The elimination half-life (t_{1/2el}) was calculated by the formula ln2/k_{el} and the mean residence time (MRT), representing the average time that a molecule stays in the body, was estimated as the ratio between the area under the first moment curve and the correspondent AUC_{0-t}. The percentage of the AUC that was extrapolated (AUC_{extrap} (%)) from the time of the last quantifiable drug concentration to infinity was also calculated as [(AUC_{inf} - AUC_{0-t})/AUC_{inf}] × 100. This parameter that should be inferior to 20% to guarantee that the sampling schedule was appropriate.

Plasmatic absolute bioavailability (F) and relative bioavailability (F_{rel}) of PER after oral administration of a suspension and after IN administration through FH5 and FO1.2 were calculated as follows (equation (1) and (2)):

$$F = \frac{AUC_{inf-oral} \times Dose_{IV}}{AUC_{inf-IV} \times Dose_{oral}} \times 100 \quad (1)$$

$$F_{rel} = \frac{AUC_{inf-oral} \times Dose_{oral}}{AUC_{inf-oral} \times Dose_{oral}} \times 100 \quad (2)$$

To evaluate the extend of PER exposure in brain, liver and kidney after its IN administration through FH5 and FO1.2 and after IV and oral administrations, AUC_{tissue}/AUC_{plasma} ratios were calculated and compared (AUC_{0-t} was used for these calculations).

To understand the overall tendency for PER accumulation in brain after IN administration of FH5 and FO1.2 *versus* IV administration, the drug targeting efficiency percentage (DTE (%)) was calculated using dose-normalized AUC_{brain} and AUC_{plasma} values (AUC_{0-t} was used for these calculations), (equation (3)):

$$DTE (\%) = \frac{\left(\frac{AUC_{brain}}{AUC_{plasma}}\right)_{IN}}{\left(\frac{AUC_{brain}}{AUC_{plasma}}\right)_{IV}} \times 100 \quad (3)$$

DTE (%) values can range from -∞ to +∞, with values above 100% indicating a more efficient brain targeting through IN administration when compared with IV injection, and values below 100% indicating the opposite (Gonçalves et al., 2021; Pires and Santos, 2018).

Nose-to-brain direct transport percentage (DTP (%)) of PER that is

estimated to reach the brain through direct routes (i.e., trigeminal and olfactory nerves) was also calculated considering dose-normalized AUC_{brain} and AUC_{plasma} values (AUC_{0-t} was used for these calculations) (equation (4)):

$$DTP (\%) = \frac{AUC_{brain-IN} - \left(\frac{AUC_{brain-IV}}{AUC_{plasma-IV}} \times AUC_{plasma-IN}\right)}{AUC_{brain-IN}} \times 100 \quad (4)$$

DTE (%) values can theoretically range from -∞ to 100%, where values below zero indicate a more efficient drug delivery to brain by systemic routes rather than direct routes. With positive DTP values, the occurrence of direct delivery of PER from nasal cavity to brain can be assumed, with higher positive values representing an increased contribution of direct routes to brain delivery (Gonçalves et al., 2021; Pires and Santos, 2018).

Comparative PER brain bioavailability between IN and IV routes (% B_{brain IN/IV}) was also calculated considering brain AUC_{0-t} dose-normalized values. This enables to determine brain PER accumulation through IN route over the IV route without considering plasma AUC_{0-t} values:

$$\%B_{brain IN/IV} = \frac{AUC_{brain-IN}}{AUC_{brain-IV}} \times 100 \quad (6)$$

Values above 100% indicate a higher drug accumulation in the brain after IN administration than after IV injection.

In vivo pharmacokinetic data were expressed as mean ± standard error of the mean (SEM) and a two-way ANOVA analysis with Tukey's multiple comparisons *post-hoc* test was applied to determine statistical differences among the two IN formulations, the IV (dose-normalized concentrations *vs* time) and oral administrations. A two-way ANOVA analysis with Dunnett's *post-hoc* test was applied when tissue-to-plasma ratios of IN and oral routes were compared with tissue-to-plasma ratios obtained with IV administration, with IV results used as control.

2.4.7. In vivo histopathological toxicity assessment

The toxicity in the nasal mucosa of FH5 and FO1.2 containing 6 mg/mL of PER was evaluated by histopathology using the periodic acid–Schiff (PAS) staining. For comparison, formulations not loaded with PER were also tested [FH5(-PER) and FO1.2(-PER)]. Systemic toxicity was evaluated by staining the major organs (brain, heart, lungs, liver and kidneys) with hematoxylin and eosin (H&E). For that, 24 adult CD-1 mice were randomly assigned to 6 groups (n = 4), anesthetized, and intranasally administered with 5 μL/30 g body weight of negative control (NaCl 0.9% solution), positive control [sodium deoxycholate 1% (w/v)] (Bae et al., 2019; Wen et al., 2011), FH5, FH5(-PER), FO1.2 or FO1.2(-PER) once a day during 7 consecutive days. Animal weight was controlled every day before administration. Twenty-four hours after the last administration, mice were sacrificed by cervical dislocation followed by decapitation. Organs and nasal cavities were carefully excised to avoid any damage and fixed with 10% neutral buffered formalin for 72 h. Tissues were dehydrated in a graded series of ethanol and then embedded in paraffin. Paraffin blocks were horizontally cut in 5 μm thick tissue sections using a micrometer and stained either with PAS (nasal cavities) or H&E (organs) to be examined using an optical microscope (Axio Imager A1, Carl Zeiss, Oberkochen, Germany).

3. Results

3.1. Pharmaceutical characterization of intranasal formulations

3.1.1. Viscosity, pH, mean particle size and polydispersity index

Considering the high lipophilicity of PER, several formulations were prepared and PER solubility was determined in each one (Supplementary Tables S1 and S2). Then, based on the solubility values and preliminary *in vivo* results (data not shown), two IN formulations – FH5 and FO1.2 – were selected for a more extensive pharmaceutical and

pharmacokinetic characterization. By visual observation of formulations FH5 and FO1.2, loaded or not with PER, both were clear, colorless and without visible particles or aggregates. These characteristics were maintained even after 2 weeks stored at room temperature and protected from light. A Newtonian-fluid behavior was observed in both formulations. Viscosity was higher in FH5 (110.50 ± 1.05 mPa·s) than in FO1.2 (15.29 ± 0.22 mPa·s) and an increase in the viscosity value (approximately 1.3-fold) was observed when FH5 was loaded with PER at 6 mg/mL. The viscosity value of FO1.2 equally increased when PER was added at that same concentration. FH5 has only 10% water but is water dispersible, behaving like a self-emulsifying drug delivery system, in this case as a SMEDDS. So, upon dispersion in water (25- and 100-fold dilutions), FH5 originated nanodroplets homogeneously distributed (PDI of 0.060 ± 0.001) with a mean size of 20.07 ± 0.03 nm. Considering the hydrophobic character of FO1.2, the measurement of droplet size and PDI was not possible since its dispersion in water was not achievable. It was also not possible to measure the pH of FO1.2 because it only has 5% of water in its composition and could not be dispersed in water. For FH5, the pH value measured upon dilution was 5.9 ± 0.22 , one logarithmic unit lower than the pH of the water in which FH5 was dispersed (6.9 ± 0.23), which is fairly within the physiological pH range (5.0 – 6.5) of the human nasal mucosa (Pires and Santos, 2018).

3.1.2. *In vitro* release study

PER release from FH5 and FO1.2 was evaluated using horizontal Ussing chambers. The aim was to correlate the *in vitro* PER release with the *in vivo* behavior after IN administration of both formulations to mice. Ensuring the achievement of sink conditions, PER release from FH5 and FO1.2 was compared with its release from positive (C+) and negative (C-) controls. A solution of PER prepared in Transcutol, from which it is expected to quickly occur a total drug release, was used as positive control, and a solution of PER prepared in Capryol 90, a hydrophobic excipient that is expected to retain PER, was used as negative control.

The profiles of PER release cumulative percentage and the PER release rates are shown in Fig. 1 and Table 1, respectively. After fitting different kinetic models to the data, the model that best fit to both formulations was the zero-order kinetic model. Therefore, the analysis was performed using linear regression (within the linear range) and the differences in release rates were compared applying an F-test. Considering the higher viscosity of FH5 compared with the one of FO1.2, it could be expected a lower PER diffusion and, consequently, a more sustained PER release from FH5. However, the opposite behavior occurred and a significant difference in PER release rates from FH5 and FO1.2 was found ($p < 0.0001$), with FO1.2 only releasing approximately 1.5% of the PER content after 4 h of assay. Given the hydrophobic

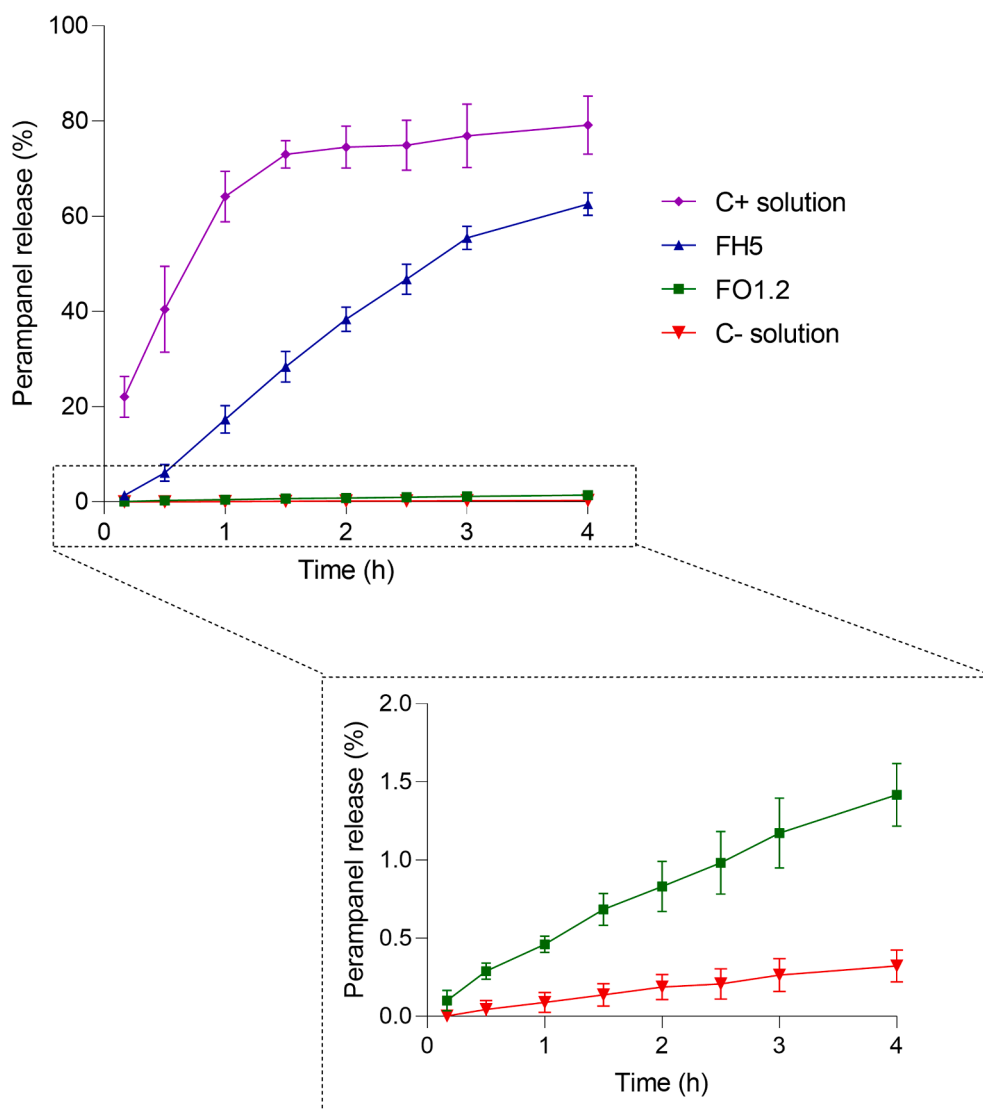


Fig. 1. Percentual release of perampanel over the 240 min of *in vitro* testing. Symbols represent the mean values \pm SEM of the four individual chambers used ($n = 4$). C+, positive control using a Transcutol solution; C-, negative control using a Capryol 90 solution.

Table 1

Release rate of perampanel (PER) in the studied formulations – FH5 and FO1.2 – and in a positive control (C+), prepared in Transcutol, and in a negative control (C-), prepared in Capryol 90. Rate constants were calculated applying a linear regression to the plots of time vs drug release percentage normalized by the area of the membrane used in the assay (0.64 cm²).

Formulation	R ²	PER release rate (%•cm ⁻² •t)	
		Mean	SD
FH5	0.997	30.63	0.728
FO1.2	0.989	0.535	0.023
C+	0.671	20.38	5.82
C + ^a	0.954	60.42	9.38
C-	0.989	0.131	0.006

^a The presented R² and rate constant values correspond only to the linear range of perampanel percentage release.

composition of the FO1.2 and the lipophilic nature of PER, a possible explanation for this could be a PER partition to the oily formulation, extensively inhibiting its diffusion through membranes into the aqueous nasal fluid simulant (receptor compartment). Nonetheless, PER release from FO1.2 was faster compared with the release from Capryol 90 solution ($p < 0.0001$). This demonstrates that, even in a lower percentage and at a slow rate, some amount of PER can be released from FO1.2 (Table 1). Given that PER is practically insoluble in water, it could also be expected that PER release from FH5 to nasal fluid simulant might be diminished. Nevertheless, even not complete, the PER release percentage was about 65%, as demonstrated in Fig. 1. Moreover, Table 1 shows that the PER release rate from FH5 was particularly high, but still significantly slower ($p = 0.0011$) than PER release from Transcutol solution (note that release rate in Transcutol solution was calculated considering only the percentage range that fits a zero-order kinetic model). This might have been due to the SMEDDS nature of FH5 that, when in contact with an aqueous environment as nasal fluid simulant or *in vivo* nasal mucosa, immediately auto-emulsifies, trapping PER into the oil droplets formed. Then, PER can either be transported through the membranes inside the droplets, or droplets allow a faster diffusion of PER to the aqueous phase. This process can be relatively fast, as observed in the obtained results, but not so fast as if PER was solubilized and readily free to pass through membranes, as it occurs in the Transcutol solution.

Thus, based on the obtained *in vitro* results, it is expected that FH5 could be more successfully applied in epilepsy treatment, since it allows a much larger and faster PER release, when compared with FO1.2. These results might help to predict the FH5 and FO1.2 behavior when administered in nasal cavities. However, physiological features must be carefully considered once they can modify the *in vitro* predicted outcomes.

3.2. Pharmacokinetic study results

The pharmacokinetic profiles of PER in mice after IV, oral, and IN administration using the hydrophobic formulation FO1.2 and the SMEDDS FH5 were herein compared. Fig. 2 represents the mean concentration–time profiles ($n = 4$) of PER in plasma, brain, liver and kidneys. Table 2 shows the pharmacokinetic parameters for each biological matrix after PER administration through IV (0.5 mg/kg), oral (1 mg/kg) and IN routes (1 mg/kg). Additionally, PER concentrations at each post-dosing time-point were compared by multiple statistical comparisons between the two IN formulations and between these formulations and those administered by the oral and IV routes (Supplementary Table S3). Since the IV dose was half of the dose administered by oral and IN routes, dose-normalized IV profiles and pharmacokinetic parameters were also calculated and are presented in Fig. 2 and Table 2, respectively.

By analyzing Fig. 2, it is evident that PER C_{max} was reached faster after IV administration than after the other tested routes. In fact, IV

delivery allowed PER to attain the mean C_{max} after 5 min in plasma, brain and kidneys, and after 10 min in liver (Table 2). This was already expected given the immediate availability of PER in systemic circulation and its fast distribution after IV dosing. Even so, using the two tested IN formulations, the t_{max} of PER was quickly attained in plasma and brain (15 min post-dosing) and after 45 min in liver and kidneys. The t_{max} of PER by oral route was reached significantly later compared with IV and IN routes (60 min in liver and 120 min in plasma and the remaining tissues, Table 2).

Comparatively to IV and IN administration routes, PER concentrations after oral dosage (1 mg/kg) were generally lower at all post-dosing time points (Fig. 2). After IV (0.5 mg/kg) and IN (1 mg/kg) dosing, identical plasma and brain concentrations–time profiles were obtained. However, after dose-normalization of the IV concentrations and of the relevant pharmacokinetic parameters (AUC_{0-t}/Dose, AUC_{inf}/Dose and C_{max}/Dose) (Table 2), it is clear that the lower plasma and brain exposure to PER after IN administration. Nevertheless, the calculated AUC_{0-t} ratios presented in Table 3 indicate that PER brain distribution after IN administration of FH5 and FO1.2 is, respectively, 1.2- and 1.1-fold higher than the brain distribution after IV PER administration. This is in accordance with Fig. 3A that shows higher brain-to-plasma ratios between 5- and 45-min post-dosing for both FH5 and FO1.2 formulations comparatively with IV injection, even though no statistical differences were found.

The plasma AUC_{0-t} values observed after IN administration of FH5 and FO1.2 were, respectively, 1.4- and 1.1-fold higher than PER plasma exposure after oral dosing. Likewise, when brain AUC_{0-t} values are compared, the brain exposure demonstrates to be 1.6- and 1.2-fold higher with FH5 and FO1.2 than after oral administration. Lower brain-to-plasma ratios of PER after oral administration were observed in practically all time-points, particularly relatively to IN FH5 formulation (Fig. 3A). In opposition, at almost all tested time-points until 60 min, liver-to-plasma and kidney-to-plasma ratios (Fig. 3B and C) were significantly higher for oral route than for the other tested routes. This data was corroborated by the oral liver/plasma and kidney/plasma AUC_{0-t} ratios (Table 3), suggesting a faster accumulation of PER in liver and kidneys after oral dosing than after IN administration.

Comparing both IN formulations, the levels of PER after FH5 administration were constantly higher in all mice matrices than those obtained after FO1.2 instillation, with statistical differences identified at several post-dosing time points (Supplementary Table S3). FH5 yielded a C_{max} 1.9-fold higher in brain (93.87 ng/g vs 50.32 ng/g) and 1.7-fold higher in plasma (346.5 ng/mL vs 204.1 ng/mL) than FO1.2 (Table 2). These values are in accordance with PER total exposure given by AUC_{0-t} and AUC_{inf} which were, respectively, 1.2- and 1.3-fold higher in plasma and brain after FH5 administration compared with FO1.2 (Table 2). Similar patterns were observed for PER exposure in liver and kidney comparing FH5 and FO1.2 IN administration (Fig. 2C and D; Table 2). The elimination of PER was similar with both formulations, as suggested by the similar k_{el} and t_{1/2el} values in all matrices when comparing FH5 and FO1.2. The only exception was the k_{el} and t_{1/2el} obtained in liver after FO1.2 administration (0.206 h⁻¹ and 3.37 h) compared with those same values obtained with FH5 administration (0.318 h⁻¹ and 2.18 h) (Table 2), indicating a slower PER elimination from this organ when administered as FO1.2. This is consistent with the obtained MRT values in liver of 5.08 h with FO1.2 administration vs 3.27 h with FH5 IN administration (Table 2).

After IN administration of both formulations, the PER absolute bioavailability was 55.50% for FH5 and 44.65% for FO1.2 (Table 3). The calculated DTE (116.3% and 107.9% for FH5 and FO1.2, respectively) and DTP (14.03% for FH5 and 7.35% for FO1.2) values suggest a somewhat good nose-to-brain targeting/direct transport to the brain, which is also supported by the comparative values of PER brain bioavailability between IN and IV routes (63.75% for FH5 and 47.08% for FO1.2 - Table 3). In all cases, estimated pharmacokinetic parameters demonstrated to be slightly higher for FH5 than FO1.2. A significant

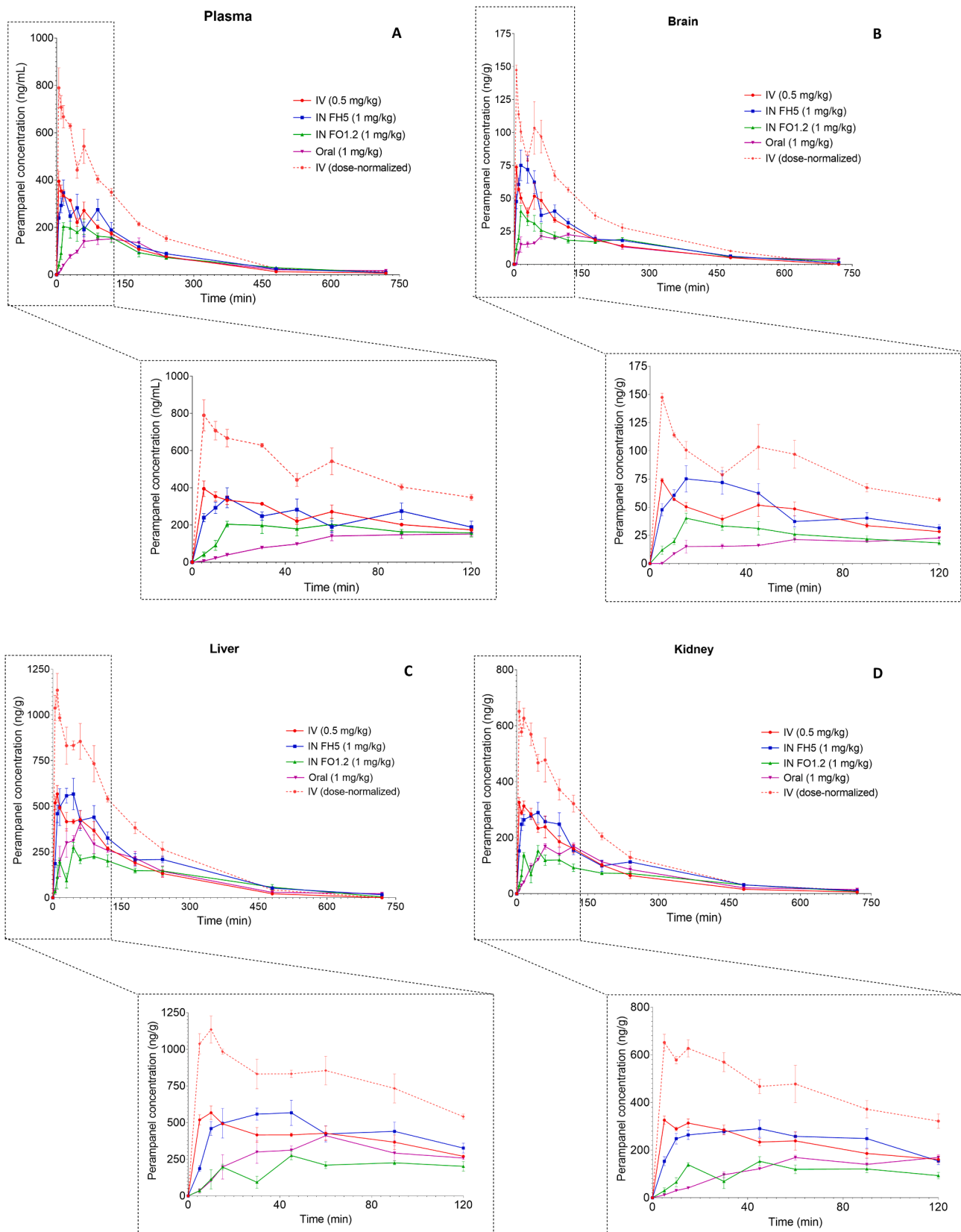


Fig. 2. Concentration-time profiles of perampanel up to 720 min post-dosing in plasma (A), brain (B), liver (C) and kidneys (D) following intravenous (IV, 0.5 mg/kg; IV, dose-normalized), oral (1 mg/kg) and intranasal (IN, FH5 and FO1.2 at 1 mg/kg) administrations to mice. Symbols represent the mean values \pm SEM of four determinations per time point (n = 4).

Table 2
Pharmacokinetic parameters of perampanel in plasma, brain, liver and kidney tissues following intranasal (IN) administration of FH5 and FO1.2 formulations (1 mg/kg) and after oral (1 mg/kg) and intravenous (IV, 0.5 mg/kg) administration to mice. Dose-normalized pharmacokinetic parameters of perampanel after IV administration are also presented.

Pharmacokinetic parameters ^a	Plasma				Brain				Liver				Kidney												
	IN - FH5		IN - FO1.2		IV		Oral		IN - FH5		IN - FO1.2		IV		Oral		IN - FH5		IN - FO1.2		IV		Oral		
	15	15	15	15	5	5	5	120	15	15	15	15	45	45	45	45	45	45	45	45	5	5	5	120	
t_{max} (min)	346.5	204.1	394.8	151.3	729.5	729.5	729.5	93.87 ^b																	
C_{max} (ng/mL)	1039	827.1	948.1	726.1	1896	1896	1896	257.7 ^c																	
$C_{max}/Dose$ (ng/mL)/(mg/kg) ^d	1073	862.9	966.4	800.2	1933	1933	1933	267.4 ^c																	
AUC_{0-t} (ng.h/mL)	3.10	4.15	1.89	9.27	0.284	0.284	0.284	3.60	3.60	3.60	3.60	3.60	3.60	3.60	3.60	3.60	3.60	3.60	3.60	3.60	3.60	3.60	3.60	3.60	3.60
$AUC_{0-t}/Dose$ (ng.h/mL)/(mg/kg) ^d	2.44	2.72	1.93	3.04	2.44	2.44	2.44	2.56	2.56	2.56	2.56	2.56	2.56	2.56	2.56	2.56	2.56	2.56	2.56	2.56	2.56	2.56	2.56	2.56	2.56
AUC_{extrap} (%)	3.19	3.77	2.63	4.80	3.39	3.39	3.39	4.32	4.32	4.32	4.32	4.32	4.32	4.32	4.32	4.32	4.32	4.32	4.32	4.32	4.32	4.32	4.32	4.32	4.32
k_{el} (h ⁻¹)	3.10	4.15	1.89	9.27	0.284	0.284	0.284	3.60	3.60	3.60	3.60	3.60	3.60	3.60	3.60	3.60	3.60	3.60	3.60	3.60	3.60	3.60	3.60	3.60	3.60
$t_{1/2el}$ (h)	2.44	2.72	1.93	3.04	2.44	2.44	2.44	2.56	2.56	2.56	2.56	2.56	2.56	2.56	2.56	2.56	2.56	2.56	2.56	2.56	2.56	2.56	2.56	2.56	2.56
MRT (h)	3.19	3.77	2.63	4.80	3.39	3.39	3.39	4.32	4.32	4.32	4.32	4.32	4.32	4.32	4.32	4.32	4.32	4.32	4.32	4.32	4.32	4.32	4.32	4.32	4.32

^a Parameters were estimated using the mean concentration–time profiles obtained from four animals per time point ($n = 4$).

^b Values expressed in ng/g.

^c Values expressed in ng.h/g.

^d Dose-normalized pharmacokinetic parameters calculated for the different matrices considering an IV administration dose of 0.5 mg/kg. AUC_{0-t} area under the concentration–time curve from time zero to infinity; C_{max} maximum (peak) concentration; last quantifiable drug concentration; AUC_{extrap} extrapolated area under drug concentration–time curve from time zero to infinity; $t_{1/2el}$ elimination half-life; t_{max} time to reach maximum (peak) concentration; k_{el} , terminal elimination rate constant; MRT, mean residence time; $t_{1/2el}$, elimination half-life; t_{max} , time to reach maximum (peak) concentration.

improvement of PER nasal systemic absorption compared to the oral route is also revealed by the calculated relative bioavailability of 134.1% and 107.8% for FH5 and FO1.2, respectively (Table 3).

3.3. *In vivo* histopathological toxicity assessment

Aiming to assess the local and systemic safety profiles of both IN formulations (FH5 and FO1.2) loaded or not with PER, a histopathological evaluation of mice nasal mucosa and major organs (brain, heart, lungs, liver and kidneys) was performed after a 7-day repeated dose study, as described in section 2.4.7. Signs of toxicity were evaluated by a trained pathologist and representative histological sections of nasal mucosa and solid organs are shown in Fig. 4. Overall, local toxicity in nasal cavities was not observed, with no signs of nasal mucosa damage detected after the IN administration of both FH5 and FO1.2, loaded or not with PER. Contrary to what occurred in mice dosed with positive control [sodium deoxycholate 1% (w/v)], the IN formulations (FO1.2 and FH5) did not cause any signs of separation between pseudostratified columnar epithelium and the basement membranes, with only minimal presence of desquamated cells in nasal cavity. In fact, these results were comparable to those obtained in mice treated with NaCl 0.9% (negative control). In general, the nasal cavities of all animals, including the ones of negative control group (NaCl 0.9%), presented diffuse findings of thickening and congestion in the interalveolar septa and a minimal decrease in the number of goblet cells. Curiously, these histopathological changes were less evident in one animal of the FH5(-PER) group, in three animals of FH5 group and in one animal of the FO1.2 group. This might be an indication of some spontaneous chronic inflammation, possibly linked with the inhaled dust present in the housing cages and not with the formulations and/or PER itself. Regarding systemic toxicity, no histopathological changes were detected in brain, heart and kidneys of mice belonging to different groups. In liver, some variability between animals was observed, particularly regarding glycogen accumulation foci present in some mice livers. This finding can be caused by multiple endogenous factors, as diet and metabolism, and also be linked to drug hepatotoxicity. However, since these findings are also present in positive and negative control groups, a relationship with PER toxicity can be excluded. Concerning mice lungs, there were no signs of histopathological alterations in this organ structure, also without signs of protein material accumulation that usually occurs when exogenous substances are deposited in lungs.

4. Discussion

The direct nose-to-brain delivery of PER after IN administration, and the possibility of using this alternative route to administrate PER was herein investigated. Considering the maximum formulation volume able to be accommodated in both mouse nostrils (24 μ L) (Kapoor et al., 2016), the high PER potency demonstrated by its low plasma therapeutic concentrations in humans (0.1 – 1 μ g/mL) (Reimers and Berg, 2018), and the PER anticonvulsant activity in different epilepsy mouse models (Food and Drug Administration, 2012; Hanada et al., 2011; Rogawski and Hanada, 2013), a dose of 1 mg/kg delivered in only 5 μ L/30 g mouse body weight was herein tested for the development of a formulation suitable for IN administration of PER. To attain this objective, a formulation capable of solubilizing PER at the concentration of 6 mg/mL was required.

After several solubility assays and *in vivo* preliminary studies, two lipid-based formulations of PER were characterized and chosen for IN administration, one of hydrophobic character (FO1.2) and the other a hydrophilic SMEDDS (FH5). Given the lipophilic nature and potency of PER, both formulations allowed a significant drug strength. Additionally, by the fact that FH5 is considered a SMEDDS, it may be able to protect PER against chemical or enzymatic degradation, susceptible to occur in nasal cavity in which drug-metabolizing isoenzymes are presented (e.g. CYP3A4) even though at lower extent than in intestine or

Table 3

Calculated pharmacokinetic parameters of peramppanel after the intranasal (IN) administration of FH5 and FO1.2 (1 mg/kg), oral (1 mg/kg) and intravenous (IV, 0.5 mg/kg) administration to mice.

	F (%)	F _{rel} (%)	AUC _{0-t} ratios			DTE (%)	DTP (%)	%B _{brain IN/IV}
			Brain/plasma	Liver/plasma	Kidney/plasma			
IN - FH5	55.50	134.1	0.248	2.422	1.309	116.3	14.03	63.75
IN - FO1.2	44.65	107.8	0.230	1.677	0.995	107.9	7.354	47.08
IV	–	–	0.213	2.031	1.154	–	–	–
Oral	41.40	–	0.221	2.462	1.326	–	–	–

%B_{brain IN/IV}, comparative peramppanel brain bioavailability between intranasal and intravenous routes; AUC_{0-t}, area under the concentration time-curve from time zero to the time of the last quantifiable drug concentration; DTE, drug targeting efficiency; DTP, direct transport percentage; F, absolute bioavailability; F_{rel}, relative bioavailability; IV, intravenous.

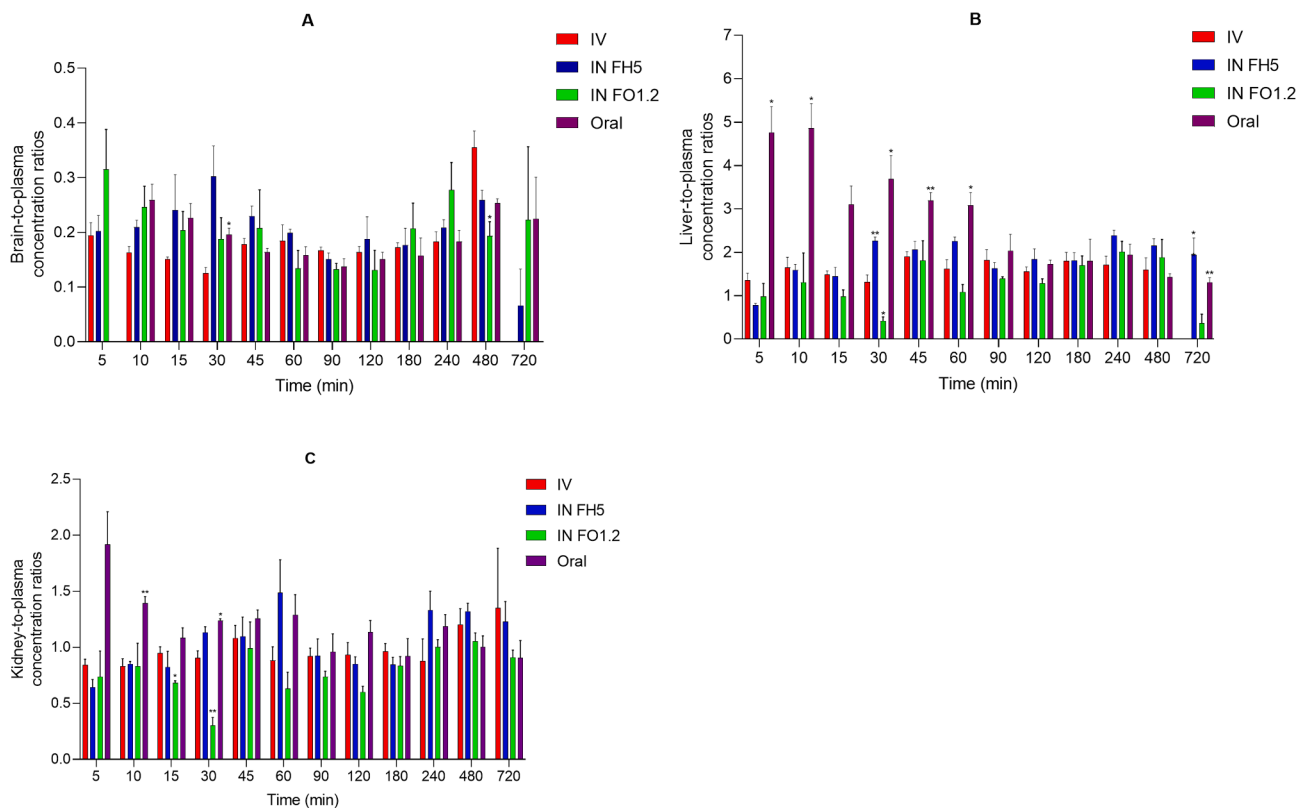


Fig. 3. Brain-to-plasma (A), liver-to-plasma (B) and kidney-to-plasma concentration ratios of peramppanel at 5, 10, 15, 30, 45, 60, 90, 120, 180, 240, 480 and 720 min after drug administration by intravenous (IV), oral and intranasal (IN, FH5 and FO1.2). Statistical differences were calculated using the IV route as control using a two-way ANOVA analysis followed by a Dunnett's post-hoc test (* $p < 0.05$, ** $p < 0.01$).

liver (Gupta et al., 2013; Oliveira et al., 2016). FH5 also presented a non-toxic pH that is in accordance with nasal cavity pH range (5.5–6.5) (Kapoor et al., 2016). Compared to nano and microemulsions, this SMEDDS formulation strategy secures maximal physical stability of the formulation. Furthermore, the presence of surfactants and the possibility of FH5 forming a microemulsion upon dispersion in the nasal mucous is expected to facilitate PER diffusion across the nasal membranes, reaching the bloodstream and brain more efficiently (Nagaraja et al., 2021; Yan et al., 2020). The higher viscosity of FH5 than FO1.2 can decrease formulation mucociliary clearance, allowing an increase of PER residence time in nasal cavity. Also, the viscosity obtained for FH5 can be sufficiently low to ensure an easy handling, packaging and flow during IN administration. Thus, the higher release rate of PER from FH5 together with its higher viscosity might help to explain PER higher bioavailability comparatively with the obtained with FO1.2. However, it must be considered that, upon FH5 dispersion in the mucous, the resultant osmolality may be very high, attracting water from the mucosa and increasing mucociliary clearance.

Considering the results of *in vitro* release kinetics (Table 1 and Fig. 1), clear differences were found when comparing them with the *in vivo* bioavailability results of PER after IN administration of FH5 and FO1.2. Actually, lipophilic drugs such as PER can be incorporated into phospholipidic bilayers of cell membranes, diffuse through them and transverse cytoplasm by rapid diffusion, with the rate of this transcellular passage enhancing as drug lipophilicity increases (Oliveira et al., 2016). The large surface area and vascularization of nasal cavity, the slower mucous layer turnover rate in olfactory region than the one in respiratory region (Crowe et al., 2018; Kapoor et al., 2016), as well as other important physiological features must also be considered when comparing *in vitro* drug release with *in vivo* results. So, all these differences between the synthetic and biological membranes could contribute to explain the obtained differences between the *in vitro* PER release assays and the extend of *in vivo* exposure, particularly after FO1.2 IN administration. The other anatomical and physiological features inherent to animals and humans must also be considered for additional explanations.

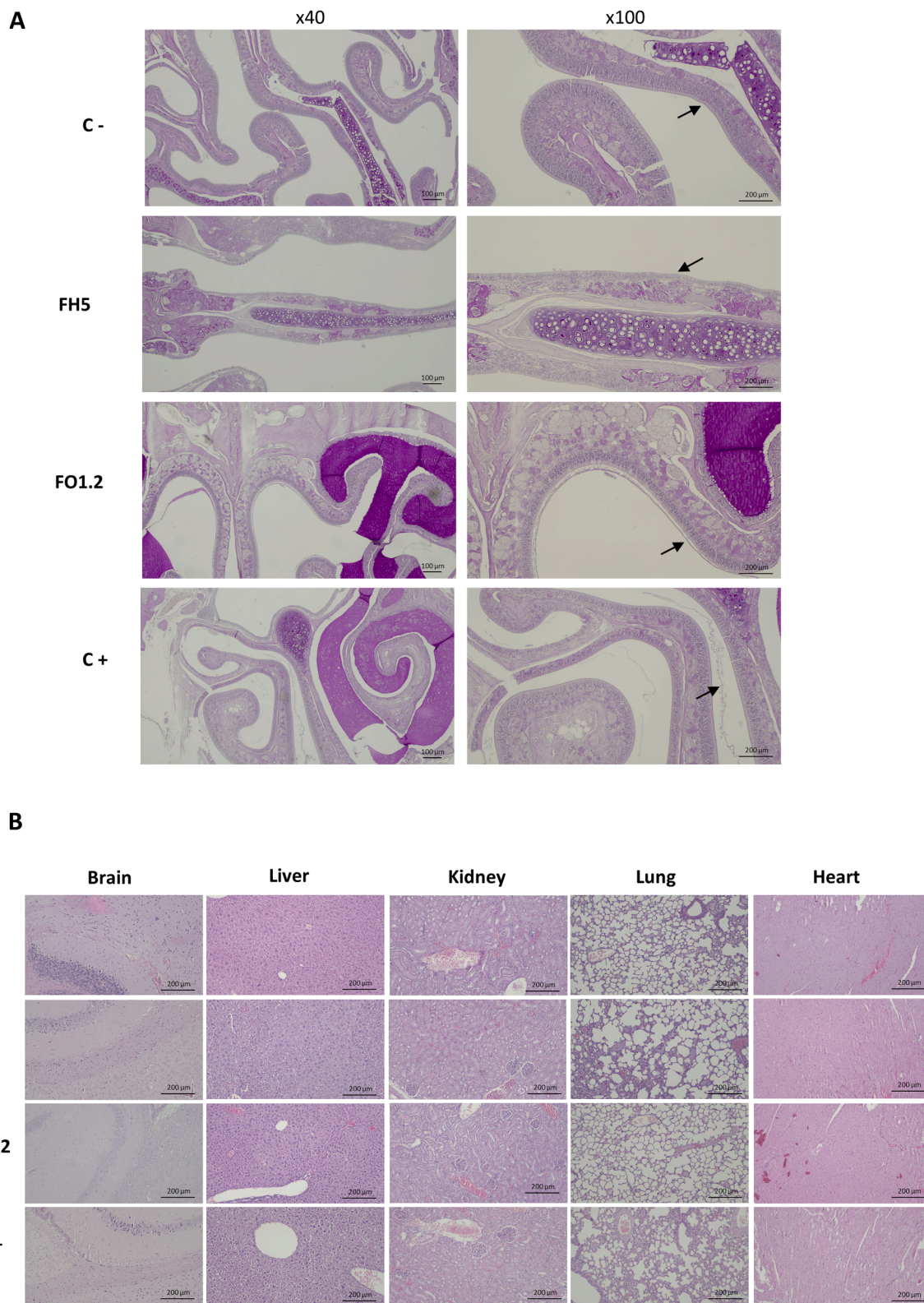


Fig. 4. *In vivo* toxicity assessed by histopathology evaluation of nasal mucosa (A) and main organs (B) after intranasal administration of formulations FH5 and FO1.2 containing 6 mg/mL of perampanel (PER), NaCl 0.9% solution (negative control - C-) and sodium deoxycholate 1% (w/v) (positive control - C+) to mice treated with each condition once a day for 7 consecutive days (n = 4). Representative images were captured by an optical microscope at x40 and x100 magnification (for main organs only x100 images are presented). Mucociliary epithelium is indicated by black arrows. There was no epithelium destruction nor inflammatory infiltration that suggested formulation and drug toxicity. Main organs were unremarkable, namely liver, heart, kidneys, and brain. On lung examination there was focal thickening of the alveolar septa and some vascular congestion, but without differences between groups.

After IN administration of PER to mice, an incomplete nasal absorption of PER occurred, explaining the absolute bioavailability obtained after FH5 and FO1.2 IN administrations. Even though, evident differences between the pharmacokinetics of both tested IN formulations can be observed, particularly in total plasma and brain exposure and its corresponding C_{max} , which is consistent with *in vitro* release kinetic studies. In fact, being FH5 a SMEDDS, by self-emulsification when in contact to nasal mucous, it could originate a higher absorption of PER (Gupta et al., 2013; Yan et al., 2020). Contrary, with FO1.2 IN administration, the high octanol–water partition coefficient of PER ($\log P$ 3.7) must be considered, which might ensure a higher affinity of PER for hydrophobic phases (Law et al., 2018). For that, a strong linking of PER to the FO1.2 oil molecules may occur, lowering its absorption either directly to brain or to the lymphatic/bloodstream, decreasing PER total bioavailability when compared with FH5 IN administration. Nevertheless, it must be considered that both formulations were probably instilled near the posterior olfactory region. This is a less ciliated region and richer in olfactory nerves than the respiratory one, minimizing the mucociliary clearance of formulations and encouraging a higher direct drug transport through the olfactory pathway (Costa et al., 2021; Kapoor et al., 2016).

In the *in vivo* assays, pharmacokinetic parameters that directly depended on administrated doses (C_{max} , AUC_{0-t} and AUC_{inf} – Table 2) were dose-normalized to enable some degree of comparability between the three different administration routes. Even though PER C_{max} in brain and plasma were reached later after IN administration than after IV dosing, a t_{max} of 15 min post IN instillation was accomplished, contrary to the late t_{max} of 120 min obtained after PER oral administration (Table 2). Considering that in the treatment of *status epilepticus* there is an overriding urgency to stop seizures before the 30 min mark (American Epilepsy Society, 2016), the IN administration of PER using FH5 and FO1.2 is a possible alternative for the management of this condition. Furthermore, if a drug can be intranasally administered 5 min after the beginning of a seizure, the need for hospitalization might decrease and time would be saved, with fewer risks of neurological damage (American Epilepsy Society, 2016; Marawar et al., 2018). Bearing in mind the PER therapeutic range (Reimers and Berg, 2018), apparently, both IN formulations could allow PER to quickly reach plasma therapeutic levels. In fact, after IN administration of FH5 to mice, PER plasma concentrations were maintained within therapeutic range up to 4 h post-dose. The brain/plasma AUC_{0-t} ratios of PER following IN administration demonstrated to be higher than the obtained by IV route (0.25 for FH5 and 0.23 for FO1.2 vs 0.21 for IV and 0.22 for the oral route, Table 3). The higher brain-to-plasma ratios obtained for both FH5 and FO1.2 formulations between 5- and 45-min post-dosing (Fig. 3) might also suggest that, during that time period, another route rather than the systemic circulation could be responsible for the PER targeting to the brain. That can be supported by DTE and DTP calculated values presented in Table 3. After 45 min post-dosing, the evolution of brain-to-plasma ratios after PER IN and IV administrations are almost parallel (Fig. 3A). This can suggest a PER targeting to brain tissue through systemic absorption and BBB crossing at later time-points. So, considering that a proportion of PER was directly delivery to brain after its IN instillation, this may also suggest an advantage in using IN administration of PER in chronic epilepsy therapy. For that, there might be a need for two administrations per day to achieve a potential control of the pathology. Interestingly, despite the drug molecules size, studies suggest that in mice the length of olfactory (~4 mm) and trigeminal (~20 mm) nerves make molecules to take about 0.74 to 2.67 h to be transported across olfactory nerve and between 17 and 56 h to diffuse along trigeminal nerves (Crowe et al., 2018). Since PER concentrations in the brain were quantified up to 12 h post-dosing, it can be hypothesized that PER directly reach brain through olfactory pathways. This is also consistent with the formulations' instillation in the most posterior zone of the mice nasal cavities. However, further specific biodistribution and pharmacodynamic studies after IN administration of PER should be

performed hereafter to clarify this issue.

Finally, the assessment of local and systemic toxicity by means of histopathological examinations of nasal mucosa and major organs (brain, liver, kidney, lungs and heart) highlighted the safety of both FH5 and FO1.2 IN formulations as suitable alternatives to the oral administration. The 7-day repeated dose study was of major importance since it is often pointed out the potentially toxic effects of some excipients used in the preparation of micro and nanoemulsions. That toxicity is frequently translated in serious mucosal irritation, itching and, in some severe cases, local pain usually related with mucosal damage and epithelium or local nervous terminations damage. However, with both tested formulations, it was not found neither mucosal damages nor changes in the integrity of pseudostratified columnar epithelium and basement membrane. There was also no decrease in goblet cells number after treatment with FH5 and FO1.2 (Fig. 4). These results show a high biocompatibility of both prepared formulations with nasal cavity. It was also demonstrated that PER itself neither induces toxicity in the administration site nor systemically after intranasally administrated using FH5 and FO1.2. Hence, FH5 and FO1.2 can be considered nontoxic nasal formulations and possible alternatives to safely administer PER in epilepsy patients.

5. Conclusions

Considering all the findings of the present study, the potential clinical relevance of nose-to-brain PER delivery strategy was herein demonstrated, particularly using FH5 as an IN formulation. Pharmaceutical characterization of FH5 revealed that it acts as a SMEDDS, with ideal values of droplet size, PDI and pH after dilution in an aqueous environment. Furthermore, *in vitro* release studies also demonstrated promising results that were further extrapolated to the obtained *in vivo* findings in mice. The IN administration of PER using FH5 revealed the highest brain/plasma AUC_{0-t} ratio, confirming that IN administration allows a high brain exposure than the oral route. In addition, the maximum PER concentration in the brain was significantly higher and reached faster through IN than with oral administration. Moreover, plasma therapeutic levels of PER were achieved at 5 min after the IN administration, and maintained until at least 4 h post FH5 dosing. No signs of local or systemic toxicity were found after administration of any of the nasal formulations, which suggests this approach safe in chronic therapeutic regimens. Nevertheless, data herein reported was obtained on mice and it cannot be directly extrapolated to humans, as there are significant anatomical differences in the nose-to-brain pathway between humans and rodents. Thereby, the pharmacokinetic results herein generated can be a primary proof of concept to design appropriate clinical trials in this scope. That interest relies on the fact that IN delivery of PER could be a feasible alternative in chronic epilepsy therapies and a safe and reliable option as *status epilepticus* rescue therapy.

Declaration of Competing Interest

The authors declare that they have no known competing financial interests or personal relationships that could have appeared to influence the work reported in this paper.

Acknowledgements

This work was gratefully supported by Foundation for Science and Technology (FCT) for the PhD fellowship of Sara Meirinho (SFRH/BD/136028/2018). The authors also acknowledge the support provided within the scope of the CICS-UBI projects UIDB/00709/2020 and UIDP/00709/2020, financed by national funds through the Portuguese Foundation for Science and Technology/MCTES. The authors also would like to thank the support provided by FEDER funds through the “Programa Operacional do Centro” (CENTRO-01-0145-FEDER-000013). This work was also supported by operation Centro-01-0145-FEDER-

000019 - C4 Cloud Computing Competence Center, cofinanced by the ERDF through the *Programa Operacional Regional do Centro* (Centro 2020), in the scope of the *Sistema de Apoio à Investigação Científica e Tecnológica - Programas Integrados de IC&DT*.

Appendix A. Supplementary material

Supplementary data to this article can be found online at <https://doi.org/10.1016/j.ijpharm.2022.121853>.

References

- Abd-Elrasheed, E., El-Helaly, S.N., EL-Ashmoony, M.M., Salah, S., 2018. Brain targeted intranasal zaleplon nano-emulsion: in-vitro characterization and assessment of gamma aminobutyric acid levels in rabbits' brain and plasma at low and high doses. *Curr. Drug Deliv.* 15 (6), 898–906. <https://doi.org/10.2174/1567201814666171130121732>.
- Alves, G., Figueiredo, I., Castel-Branco, M., Loureiro, A., Falcão, A., Caramona, M., 2007. Simultaneous and enantioselective liquid chromatographic determination of eslicarbazepine acetate, S-licarbazepine, R-licarbazepine and oxcarbazepine in mouse tissue samples using ultraviolet detection. *Anal. Chim. Acta* 596 (1), 132–140. <https://doi.org/10.1016/j.aca.2007.05.056>.
- American Epilepsy Society, 2016. Treatment of prolonged seizures in children and adults. <https://www.aesnet.org/clinical-care/clinical-guidance/guideline-prolonged-seizures> (accessed 6 January 2022).
- Bae, H.-D., Lee, J.-S., Pyun, H., Kim, M., Lee, K., 2019. Optimization of formulation for enhanced intranasal delivery of insulin with translationally controlled tumor protein-derived protein transduction domain. *Drug Deliv.* 26 (1), 622–628. <https://doi.org/10.1080/10717544.2019.1628119>.
- Bahadur, S., Pathak, K., 2012. Buffered nanoemulsion for nose to brain delivery of ziprasidone hydrochloride: preformulation and pharmacodynamic evaluation. *Curr. Drug Deliv.* 9, 596–607. <https://doi.org/10.2174/156720112803529792>.
- Biase, S. De, Gigli, G.L., Nilo, A., Romano, G., Valente, M., 2018. Pharmacokinetic and pharmacodynamic considerations for the clinical efficacy of perampamil in focal onset seizures. *Expert Opin. Drug Metab. Toxicol.* 15, 93–102. doi: 10.1080/17425255.2019.1560420.
- Boche, M., Pokharkar, V., 2017. Quetiapine nanoemulsion for intranasal drug delivery: evaluation of brain-targeting efficiency. *AAPS PharmSciTech* 18 (3), 686–696. <https://doi.org/10.1208/s12249-016-0552-9>.
- Bruschi, M., 2015. Mathematical models of drug release. In: Bruschi, M.L. (Ed.), *Strategies to modify the drug release from pharmaceutical systems*. Woodhead Publishing, pp. 63–86. <https://doi.org/10.1016/B978-0-08-100092-2.00005-9>.
- Bshara, H., Osman, R., Mansour, S., El-Shamy, A.E.H.A., 2014. Chitosan and cyclodextrin in intranasal microemulsion for improved brain bioactive hydrochloride pharmacokinetics in rats. *Carbohydr. Polym.* 99, 297–305. <https://doi.org/10.1016/j.carbpol.2013.08.027>.
- Chang, F.M., Fan, P.C., Weng, W.C., Chang, C.H., Lee, W.T., 2020. The efficacy of perampamil in young children with drug-resistant epilepsy. *Seizure* 75, 82–86. <https://doi.org/10.1016/j.seizure.2019.12.024>.
- Costa, C., Moreira, J.N., Amaral, M.H., Sousa Lobo, J.M., Silva, A.C., 2019. Nose-to-brain delivery of lipid-based nanosystems for epileptic seizures and anxiety crisis. *J. Control. Release* 295, 187–200. <https://doi.org/10.1016/j.jconrel.2018.12.049>.
- Costa, C.P., Moreira, J.N., Sousa Lobo, J.M., Silva, A.C., 2021. Intranasal delivery of nanostructured lipid carriers, solid lipid nanoparticles and nanoemulsions: a current overview of in vivo studies. *Acta Pharm. Sin. B* 11, 925–940. <https://doi.org/10.1016/j.apsb.2021.02.012>.
- Crowe, T.P., Greenlee, M.H.W., Kanthasamy, A.G., Hsu, W.H., 2018. Mechanism of intranasal drug delivery directly to the brain. *Life Sci.* 195, 44–52. <https://doi.org/10.1016/j.lfs.2017.12.025>.
- Der-Nigoghossian, C., Rubinos, C., Alkhachroum, A., Claassen, J., 2019. Status epilepticus - time is brain and treatment considerations. *Curr. Opin. Crit. Care* 25 (6), 638–646. <https://doi.org/10.1097/MCC.0000000000000661>.
- Erdő, F., Bors, L.A., Farkas, D., Bajza, A., Gizurarson, S., 2018. Evaluation of intranasal delivery route of drug administration for brain targeting. *Brain Res. Bull.* 143, 155–170. <https://doi.org/10.1016/j.brainresbull.2018.10.009>.
- European Medicines Agency, 2017. Perampamil (Fycompa). Summary of product characteristics 1–83. https://www.ema.europa.eu/en/documents/product-information/fycompa-epar-product-information_en.pdf (accessed 6 January 2022).
- Feng, Y., He, H., Li, F., Lu, Y., Qi, J., Wu, W., 2018. An update on the role of nanovehicles in nose-to-brain drug delivery. *Drug Discov. Today* 23 (5), 1079–1088. <https://doi.org/10.1016/j.drudis.2018.01.005>.
- Florence, K., Manisha, L., Kumar, B.A., Ankur, K., Kumar, M.A., Ambikanandan, M., 2011. Intranasal clobazam delivery in the treatment of status epilepticus. *Pharm. Nanotechnol.* 100, 692–703. <https://doi.org/10.1002/jps>.
- Fogarasi, A., Flamini, R., Millh, M., Phillips, S., Yoshitomi, S., Patten, A., Takase, T., Laurenza, A., Ngo, L.Y., 2020. Open-label study to investigate the safety and efficacy of adjunctive perampamil in pediatric patients (4 to <12 years) with inadequately controlled focal seizures or generalized tonic-clonic seizures. *Epilepsia* 61, 125–137. <https://doi.org/10.1111/epi.16413>.
- U.S. Food and Drug Administration, 2020. Valtoco - New drug application. <https://www.accessdata.fda.gov/scripts/cder/daf/index.cfm?event=overview.process&ApplNo=211635> (accessed 6 January 2022).
- Food and Drug Administration, 2012. Perampamil (Fycompa) Clinical Pharmacology and Biopharmaceutics Reviews. <https://www.accessdata.fda.gov> (accessed 6 January 2022).
- Gonçalves, J., Silva, S., Gouveia, F., Bicker, J., Falcão, A., Alves, G., Fortuna, A., 2021. A combo-strategy to improve brain delivery of antiepileptic drugs: focus on BCRP and intranasal administration. *Int. J. Pharm.* 593, 120161. <https://doi.org/10.1016/j.ijpharm.2020.120161>.
- Gupta, S., Kesarla, R., Omri, A., 2013. Formulation strategies to improve the bioavailability of poorly absorbed drugs with special emphasis on self-emulsifying systems. *Shweta. ISRN Pharm.* 2013, 1–16. <https://doi.org/10.1155/2013/848043>.
- Hanada, T., Hashizume, Y., Tokuhara, N., Takenaka, O., Kohmura, N., Ogasawara, A., Hatakeyama, S., Ohgoh, M., Ueno, M., Nishizawa, Y., 2011. Perampamil : A novel , orally active, noncompetitive AMPA-receptor antagonist that reduces seizure activity in rodent models of epilepsy 52, 1331–1340. doi: 10.1111/j.1528-1167.2011.03109.x.
- Ikemoto, S., Hamano, S.-I., Hirata, Y., Matsuura, R., Koichihara, R., 2019. Efficacy and serum concentrations of perampamil for treatment of drug-resistant epilepsy in children, adolescents, and young adults: comparison of patients younger and older than 12 years. *Seizure* 73, 75–78. <https://doi.org/10.1016/j.seizure.2019.10.023>.
- Iqbal, R., Ahmed, S., Jain, G.K., Vohora, D., 2019. Design and development of letrozole nanoemulsion: a comparative evaluation of brain targeted nanoemulsion with free letrozole against status epilepticus and neurodegeneration in mice. *Int. J. Pharm.* 565, 20–32. <https://doi.org/10.1016/j.ijpharm.2019.04.076>.
- Kapoor, M., Cloyd, J.C., Siegel, R.A., 2016. A review of intranasal formulations for the treatment of seizure emergencies. *J. Control. Release* 237, 147–159. <https://doi.org/10.1016/j.jconrel.2016.07.001>.
- Kumar, M., Misra, A., Babbar, A.K., Mishra, A.K., Mishra, P., Pathak, K., 2008a. Intranasal nanoemulsion based brain targeting drug delivery system of risperidone. *Int. J. Pharm.* 358 (1–2), 285–291. <https://doi.org/10.1016/j.ijpharm.2008.03.029>.
- LaPenna, P., Tormoehlen, L.M., 2017. The pharmacology and toxicology of third-generation anticonvulsant drugs. *J. Med. Toxicol.* 13 (4), 329–342. <https://doi.org/10.1007/s13181-017-0626-4>.
- Law, V., Knox, C., Djoumbou, Y., Jewison, T., Guo, A.C., Liu, Y., Maciejewski, A., Arndt, D., Wilson, M., Neveu, V., Tang, A., Gabriel, G., Ly, C., Adamjee, S., Dame, Z.T., Han, B., Zhou, Y., W.D., 2018. Perampamil. <https://www.drugbank.ca/drugs/DB08883> (accessed 6 January 2022).
- Li, X., Frech, F., Plauschinat, C.A., Gore, M., 2021. Real-world hospitalization risk in patients with epilepsy treated with perampamil. *Epilepsy Behav.* 114, 1–5. <https://doi.org/10.1016/j.yebeh.2020.107270>.
- Marawar, R., Basha, M., Mahulikar, A., Desai, A., Suchdev, K., Shah, A., 2018. Updates in refractory status epilepticus. *Crit. Care Res. Pract.* 2018, 1–19. <https://doi.org/10.1155/2018/9768949>.
- Meirinho, S., Campos, G., Rodrigues, M., Fortuna, A., Falcão, A., Alves, G., 2020. Salting-out assisted liquid-liquid extraction method optimized by design of experiments for the simultaneous HPLC analysis of perampamil and stiripentol in mouse matrices. *J. Sep. Sci.* 43, 4289–4304. <https://doi.org/10.1002/jssc.202000656>.
- Meirinho, S., Rodrigues, M., Fortuna, A., Falcão, A., Alves, G., 2021. Liquid chromatographic methods for determination of the new antiepileptic drugs stiripentol, retigabine, rufinamide and perampamil: a comprehensive and critical review. *J. Pharm. Anal.* 11 (4), 405–421. <https://doi.org/10.1016/j.jpha.2020.11.005>.
- Mustafa, G., Ahuja, A., Al Rohaimi, A.H., Muslim, S., Hassan, A.A., Baboota, S., Ali, J., 2015. Nano-ropinirel for the management of Parkinsonism: blood-brain pharmacokinetics and carrier localization. *Expert Rev. Neurother.* 15 (6), 695–710. <https://doi.org/10.1586/14737175.2015.1036743>.
- Nagaraja, S., Basavarajappa, G.M., Karnati, R.K., Bakir, E.M., Pund, S., 2021. Ion-triggered in situ gelling nanoemulgel as a platform for nose-to-brain delivery of small lipophilic molecules. *Pharmaceutics* 13, 1–20. <https://doi.org/10.3390/pharmaceutics13081216>.
- Newey, C.R., Mullaguri, N., Hantus, S., Punia, V., George, P., 2019. Super-refractory status epilepticus treated with high dose perampamil: case series and review of the literature. *Case Reports Crit. Care* 2019, 1–7. <https://doi.org/10.1155/2019/3218231>.
- Oliveira, P., Fortuna, A., Alves, G., Falcao, A., 2016. Drug-metabolizing enzymes and efflux transporters in nasal epithelium: influence on the bioavailability of intranasally administered drugs. *Curr. Drug Metab.* 17 (7), 628–647. <https://doi.org/10.2174/1389200217666160406120509>.
- Patsalos, P.N., 2015. The clinical pharmacology profile of the new antiepileptic drug perampamil : a novel noncompetitive AMPA receptor antagonist. *Pharmacokinetics of Perampamil in Adults. Epilepsia* 56, 12–27. <https://doi.org/10.1111/epi.12865>.
- Pires, P.C., Santos, A.O., 2018. Nanosystems in nose-to-brain drug delivery: a review of non-clinical brain targeting studies. *J. Control. Release* 270, 89–100. <https://doi.org/10.1016/j.jconrel.2017.11.047>.
- Pires, P.C., Peixoto, D., Teixeira, I., Rodrigues, M., Alves, G., Santos, A.O., 2020. Nanoemulsions and thermosensitive nanoemulgels of phenytoin and fosphenytoin for intranasal administration: formulation development and in vitro characterization. *Eur. J. Pharm. Sci.* 141, 105099. <https://doi.org/10.1016/j.ejps.2019.105099>.
- Rahbani, A., Adwane, G., Jomaa, N., 2019. Oral perampamil for the treatment of super-refractory status epilepticus. *Case Rep. Neurol. Med.* 2019, 1–3. <https://doi.org/10.1155/2019/8537815>.
- Ramreddy, S., Janapareddi, K., 2019. Brain targeting of chitosan-based diazepam mucoadhesive microemulsions via nasal route: formulation optimization, characterization, pharmacokinetic and pharmacodynamic evaluation. *Drug Dev. Ind. Pharm.* 45 (1), 147–158. <https://doi.org/10.1080/03639045.2018.1526186>.

- Rashed, H.M., Shamma, R.N., El-Sabagh, H.A., 2018. Preparation of 99m Tc-levetiracetam intranasal microemulsion as the first radiotracer for SPECT imaging of the Synaptic Vesicle Protein SV2A. *Eur. J. Pharm. Sci.* 121, 29–33. <https://doi.org/10.1016/j.ejps.2018.05.019>.
- Reimers, A., Berg, J.A., 2018. Reference ranges for antiepileptic drugs revisited: a practical approach to establish national guidelines Reference ranges for antiepileptic drugs revisited : a practical approach to establish national guidelines. *Drug Des. Devel. Ther.* 12, 271–280. <https://doi.org/10.2147/DDDT.S154388>.
- Rogawski, M.A., Hanada, T., 2013. Preclinical pharmacology of perampanel, a selective non-competitive AMPA receptor antagonist. *Acta Neurol. Scand.* 127, 19–24. <https://doi.org/10.1111/ane.12100>.
- Shah, B., Khunt, D., Misra, M., Padh, H., 2018. Formulation and In-vivo pharmacokinetic consideration of intranasal microemulsion and mucoadhesive microemulsion of rivastigmine for brain targeting. *Pharm. Res.* 35 (1) <https://doi.org/10.1007/s11095-017-2279-z>.
- Singhvi, G., Singh, M., 2011. Review: in-vitro drug release characterisation models. *Int. J. Pharm. Stud. Res.* 2, 77–84.
- Strzelczyk, A., Knake, S., Kälviäinen, R., Santamarina, E., Toledo, M., Willig, S., Rohrer, A., Trinka, E., Rosenow, F., 2019. Perampanel for treatment of status epilepticus in Austria, Finland, Germany, and Spain. *Acta Neurol. Scand.* 139 (4), 369–376. <https://doi.org/10.1111/ane.13061>.
- Toledano Delgado, R., García-Morales, I., Parejo-Carbonell, B., Jiménez-Huete, A., Herrera-Ramirez, D., González-Hernández, A., Ayuga Loro, F., Santamarina, E., Toledo, M., Ojeda, J., Poza, J.J., Molins, A., Giner, P., Estévez María, J.C., Castro-Vilanova, M.D., Zurita, J., Saiz-Díaz, R.A., Gómez-Ibañez, A., Rodríguez-Uranga, J., Gil-Nagel, A., Campos, D., Sánchez-Larsen, Á., Aguilar-Amat Prior, M.J., Mauri Llerda, J.A., Huertas González, N., García-Barragán, N., 2020. Effectiveness and safety of perampanel monotherapy for focal and generalized tonic-clonic seizures: Experience from a national multicenter registry. *Epilepsia* 61 (6), 1109–1119. <https://doi.org/10.1111/epi.16548>.
- U.S. Food and Drug Administration, 2019. Nayzilam - New Drug Application. Drugs@FDA: FDA-Approved Drugs. <https://www.accessdata.fda.gov/scripts/cder/daf/index.cfm?event=overview.process&varApplNo=211321> (accessed 6 January 2022).
- Wen, Z., Yan, Z., He, R., Pang, Z., Guo, L., Qian, Y., Jiang, X., Fang, L., 2011. Brain targeting and toxicity study of odorranalectin-conjugated nanoparticles following intranasal administration. *Drug Deliv.* 18 (8), 555–561. <https://doi.org/10.3109/10717544.2011.596583>.
- World Health Organization, 2019. Epilepsy. <https://www.who.int/news-room/fact-sheets/detail/epilepsy> (accessed 6 January 2022).
- Yan, B., Ma, Y., Guo, J., Wang, Y., 2020. Self-microemulsifying delivery system for improving bioavailability of water insoluble drugs. *J. Nanoparticle Res.* 22, 1–14. <https://doi.org/10.1007/s11051-019-4744-6>.
- Yu, D., Li, G., Lesniak, M.S., Balyasnikova, I.V., 2017. Intranasal delivery of therapeutic stem cells to glioblastoma in a mouse model. *J. Vis. Exp.* 2017, 1–9. <https://doi.org/10.3791/55845>.